Electron-impact study of the B_2 molecule using the *R*-matrix method

Jasmeet Singh Rajvanshi* and K. L. Baluja†
Department of Physics and Astrophysics, University of Delhi, Delhi 110007, India
(Received 7 November 2011; revised manuscript received 15 May 2012; published 7 September 2012)

The results of *ab initio* scattering calculations for low-energy electron collisions with the B_2 molecule using the *R*-matrix method have been presented. The differential and momentum-transfer cross sections along with effective collision frequency over a wide electron temperature range (300–30 000 K) are computed at the one-state close-coupling level. In this work, 61-state close-coupling calculations are performed to compute the integral cross sections (elastic and excitations). We investigated five resonances: two in the excitation cross sections of $A\,^3\Pi_u$, two in the excitation cross sections of $a\,^5\Sigma_u^-$ and one in both $b\,^1\Delta_g$ and $c\,^1\Sigma_g^+$ excited states. The Born correction for the dipole-allowed transition ($X\,^3\Sigma_g^-$ to $A\,^3\Pi_u$) has been carried out to account for the contribution of partial waves higher than the g wave ($l = 4$) up to which the *R*-matrix scattering calculations are carried. We have detected a stable anionic bound state $^2\Pi_u$ of B_2^- having the configuration $1\sigma_g^2\,2\sigma_g^2\,1\sigma_u^2\,2\sigma_u^2\,1\pi_u^3$. The ionization cross sections are calculated in the binary-encounter Bethe model in which Hartree-Fock molecular orbitals at a self-consistent level are used to calculate kinetic and binding energies of the occupied molecular orbitals. We have also evaluated scattering length for electron-B_2 collisions at the one-state close-coupling level ($6.8a_0$) and at the static exchange plus polarization level ($6.2a_0$).

DOI: 10.1103/PhysRevA.86.032704 PACS number(s): 34.80.Bm, 34.80.Gs, 34.80.Ht

I. INTRODUCTION

Boron and borides have many important applications such as in stable chemical insulators, high-modulus boron fiber composites, high-temperature semiconductor devices, thermoelectric power conversion [1], and high-energy density fuels [2]. Douglas and Herzberg [3] have reported experimental evidence of the existence of B_2. They observed one transition which they assigned to the $^3\Sigma_u^-$–$^3\Sigma_g^-$ transition. Dupuis and Lui [4] made extensive calculations, using large basis sets and electron correlation, for the states which were believed to give rise to the $^3\Sigma_u^-$–$^3\Sigma_g^-$ transition. They established that the ground state of B_2 was $^3\Sigma_g^-$ and found that the upper state of the $^3\Sigma_u^-$–$^3\Sigma_g^-$ transition is 2 $^3\Sigma_u^-$ rather than 1 $^3\Sigma_u^-$. Bruna and Wright [5,6] performed multireference configuration interaction calculations to determine the ionization potential of B_2 and to study strongly bound doubly excited states ($^3\Sigma_g^-$, $^3\Pi_u$, $^1\Sigma_g^-$). Langhoff and Bauschlicher [7] studied the excited states of B_2 below 45 000 cm^{-1} at the multireference configuration-interaction (MRCI) level in a $[4s\,3p\,2d\,1f]$ atomic natural orbital (ANO) Gaussian basis set. They also performed calculations employing a $[5s\,4p\,3d\,2f\,1g]$ ANO basis for the low-lying states, $X\,^3\Sigma_g^-$, $A\,^3\Pi_u$, $a\,^5\Sigma_u^-$, $b\,^1\Delta_g$, and $c\,^1\Sigma_g^+$ to assess the accuracy of the spectroscopic constants. Configuration-interaction (CI) methods were applied by Hachey *et al.* [8] to the ground state and 55 low-lying states of B_2 using a $5s\,3p$ contracted Gaussian basis set. They reported the spectroscopic constants for 53 stable states for B_2 and compared them with theoretical and experimental results for the isovalent molecules Al_2 and Ga_2. A wide range of excited states of the diatomic molecules B_2, C_2, N_2, and O_2 were investigated theoretically by Muller *et al.* [9] at multireference configuration-interaction with all singles and doubles (MRCISD) with the Davidson correction and MR-average quadratic cluster (AQCC). They evaluated the spectroscopic constants for 60 states.

The present study uses the *ab initio* *R*-matrix method to low-energy scattering by the B_2 molecule in the fixed nuclei approximation. The calculations use the UK molecular *R*-matrix code [15,16]. The *R*-matrix method has the advantage over other scattering methods in efficiently providing cross sections at a large number of scattering energies. It also has the ability to include correlation effects and give an adequate representation of several excited states of the molecule [17]. We are interested in the low-energy region ($\leqslant$10 eV) which is a favorite ground for the *R*-matrix method. The incoming electron can occupy one of the many unoccupied molecular orbitals or can excite any occupied molecular orbital as it falls into another one. These processes give rise to the phenomenon of resonances forming a negative molecular ion for a finite time before the resonance decays into energetically open channels.

Electron scattering calculations are performed at static exchange, one-state CI, and close-coupling approximation in which we have retained 61 target states in the *R*-matrix formalism. The integrated elastic, differential, and momentum-transfer cross sections for electron impact on the B_2 molecule from its ground state are reported. The excitation cross sections from the ground state to few low-lying excited states have also been calculated. We have also computed the binary-encounter-Bethe (BEB) ionization cross section [18,19]. The BEB cross sections depend only on the binding energies, kinetic energies, and occupation number of the occupied molecular orbitals of the target, and on the energy of the incident electron. The momentum transfer cross sections calculated in the *R*-matrix approximation have been used to calculate effective collision frequency over a wide electron temperature range. We have also evaluated the scattering length for electron-B_2 collisions. In this procedure we have included only the s wave, which means that only s orbitals are contributing. We must point out that the *R*-matrix approach is not the only scattering method

*Also at Keshav Mahavidyalaya, Physics and Electronics Department, University of Delhi; rajvanshi_jasmeet@yahoo.co.in
†kl_baluja@yahoo.com

that allows the *ab initio* inclusion of correlation effects and for studies of open-shell targets. The complex Kohn variational method has been successfully employed for diatomic and polyatomic targets [20].

II. METHOD

A. Theory

The R-matrix theory [21–24] is based on the division of space into an inner region and an outer region. Both regions are treated differently in accordance with the different interactions in each region. The center of the R-matrix sphere coincides with the center of mass of the molecule. When the scattering electron leaves the inner region, the other target electrons are confined to the inner region. In the present work the R-matrix boundary radius dividing the two regions was chosen to be $10a$, centered at the B_2 center of mass. This sphere encloses the entire charge cloud of the occupied and virtual molecular orbitals included in the calculation. At $10a_0$, the amplitudes of the molecular orbitals are less than $10^{-5}a_0^{-3/2}$. However, the continuum orbitals have finite amplitudes at the boundary. Inside the R-matrix sphere, the electron-electron correlation and exchange interactions are strong. Short-range correlation effects are important for accurate prediction of large-angle elastic scattering, and exchange effects are important in more general processes, not only spin-forbidden processes. A multicentered CI wave function expansion is used in the inner region. The calculation in the inner region is similar to a bound-state calculation, which involves the solution of an eigenvalue problem for $(N+1)$ electrons in the truncated space, where there are N target electrons and a single scattering electron. Most of the physics of the scattering problem is contained in this $(N+1)$ electron bound-state molecular-structure calculation. Outside the sphere, only long-range multipolar interactions between the scattering electron and the various target states are included. Because only direct potentials are involved in the outer region, a single center approach is used to describe the scattering electron via a set of coupled differential equations. The R-matrix is a mathematical entity that connects the two regions. It describes how the scattering electron enters and leaves the inner region. In the outer region, the R-matrix on the boundary is propagated outward [25,26] until the inner-region solutions can be matched with asymptotic solutions thus yielding the physical observables such as cross sections. We include only the dipole and quadrupole potentials in the outer region.

In the polyatomic implementation of the UK molecular R-matrix code [15,16], the continuum molecular orbitals are constructed from atomic Gaussian-type orbitals (GTOs) using basis functions centered on the center of gravity of the molecule. The main advantage of GTOs is that integrals involving them over all space can be evaluated analytically in closed form. However, a tail contribution is subtracted to yield the required integrals in the truncated space defined by the inner region [15].

The target molecular orbital space is divided into core (inactive), valence (active), and virtual orbitals. The target molecular orbitals are supplemented with a set of continuum orbitals, centered on the center of gravity of the molecule. The continuum basis functions used in polyatomic R-matrix calculations are Gaussian functions and do not require fixed boundary conditions. First, target and continuum molecular orbitals are orthogonalized using Schmidt orthogonalization. Then symmetric or Löwdin orthogonalization is used to orthogonalize the continuum molecular orbitals among themselves and remove linearly dependent functions [15,27]. In general and in this work, all calculations are performed within the fixed-nuclei approximation. This is based on the assumption that electronic, vibrational, and rotational motions are uncoupled.

In the inner region, the wave function of the scattering system, consisting of target plus scattering electron, is written using the CI expression:

$$\Psi_k^{N+1} = A\sum_i \phi_i^N(x_1,\ldots,x_N)\sum_j \xi_j(x_{N+1})a_{ijk} + \sum_m \chi_m(x_1,\ldots,x_N,x_{N+1})b_{mk}, \quad (1)$$

where A is an antisymmetrization operator, x_N is the spatial and spin coordinates of the Nth electron, ϕ_i^N represents the ith state of the N-electron target, ξ_j is a continuum orbital spin-coupled with the scattering electron, and k refers to a particular R-matrix state. Coefficients a_{ijk} and b_{mk} are variational parameters determined as a result of the matrix diagonalization. To obtain reliable results, it is important to maintain a balance between the N-electron target representation, ϕ_i^N, and the $(N+1)$-electron wave function for scattering. The summation in the second term of Eq. (1) runs over configurations χ_m, where all electrons are placed in target-occupied and virtual molecular orbitals. The choice of appropriate χ_m is crucial in this [28]. These are known as L^2 configurations and are needed to account for orthogonality relaxation and for correlation effects arising from virtual excitation to higher electronic states that are excluded in the first expansion. We have included about 1800 L^2 configurations in our 61-state CI model and the same in the 1-state CI model. The basis for the continuum electron is parametrically dependent on the R-matrix radius and provides a good approximation to an equivalent basis of orthonormal spherical Bessel functions [29]. In the 1-state CI model, we have included the ground state only but have used the CI wave function to describe it. In the 61-state model calculation, each target state is represented by a CI wave function.

B. B_2 target and scattering model

The molecule B_2 is an open-shell system that has ground state $X\,^3\Sigma_g^-$ in the $D_{\infty h}$ point group which is reduced to the D_{2h} point group when the symmetry is lowered. The point group D_{2h} is the highest Abelian group in our codes. The results are reported in the natural symmetry point group as well as in the D_{2h} point group for the sake of convenience. We used a double-ζ plus polarization (DZP) Gaussian basis set [30] contracted as (9,5,1)/(4,2,1) for B. We avoided using diffuse functions, because these would extend outside the R-matrix box, which may cause linear dependency problems. We first performed a self-consistent field (SCF) calculation for the ground state of the B_2 molecule with the chosen DZP basis set and obtained a set of occupied and a set of virtual orbitals.

TABLE I. Properties of the B_2 target, ground-state energy (in a.u.), ionization potential (I.P., in eV) and the rotational constant (B_e, in cm^{-1}), SCF at bond length $R_e = 3.1021a_0$, and CI at bond length $R_e = 3.18a_0$.

	Present work		Previous results[a] ($R_e = 3.0\ a_0$)		Previous results[b] ($R_e = 3.2\ a_0$)	
	SCF	CI	SCF	CI	SCF	VCI
E	−49.0785	−49.1748	−49.090394	−49.104398	−49.0839	−49.2766
I.P.	9.54	9.36			7.29	8.81
B_e	1.136	1.081	1.17			

[a]Dupuis and Liu [4].
[b]Bruna and Wright [6].

The Hartree-Fock electronic configuration for the ground state is $1\sigma_g^2\ 2\sigma_g^2\ 1\sigma_u^2\ 2\sigma_u^2\ 1\pi_u^2$ which gives rise to lowest-lying $X\ ^3\Sigma_g^-$, $b\ ^1\Delta_g$, and $c\ ^1\Sigma_g^+$ states. The energy of the occupied $1\pi_u$ orbital is −9.54 eV and by Koopman's theorem it is the first ionization energy. Since the SCF procedure is inadequate in providing a good representation of the target states, we improve the energy of the ground as well as the excited states by using CI wave functions. A CI approach is energetically superior to a calculation based on the SCF model. This lowers the energies, and the correlation introduced provides a better description of the target wave function and excitation energies. This also gives a better description of the charge density, which is important in determining quadrupole and transition moments of the transition in the target states. In our limited CI model, we keep four electrons frozen in the $1\sigma_g^2 1\sigma_u^2$ configuration and allow the remaining six electrons to move freely in molecular orbitals $2\sigma_g$, $3\sigma_g$, $4\sigma_g$, $2\sigma_u$, $3\sigma_u$, $4\sigma_u$, $1\pi_u$, and $1\pi_g$. The CI ground-state energy for the B_2 molecule is −49.1748 hartrees, at a bond length of $R_e = 3.18\ a_0$.

To provide additional information on the charge distribution in the B_2 molecule, we also calculated the quadrupole moment. In our CI model the absolute values of quadrupole component Q_{20} for the ground state is 0.202 a.u. The values of the ground-state energy, ionization potential, and rotational constant are compared with other work in Table I.

In Table II, we list the quadrupole moment of each state (Q_{20}), N the number of configuration state functions (CSFs), and the vertical excitation energies (VEEs) for the target states. We have good agreement with the VEE calculations of Refs. [7–9].

We have included 61 target states (5 of ^1A_g, 2 of ^3A_g, 2 of ^5A_g, 4 of $^3B_{2u}$, 2 of $^1B_{2u}$, 1 of $^5B_{2u}$, 4 of $^3B_{3u}$, 2 of $^1B_{3u}$, 1 of $^5B_{3u}$, 5 of $^3B_{1g}$, 2 of $^1B_{1g}$, 2 of $^5B_{1g}$, 4 of $^3B_{1u}$, 2 of $^1B_{1u}$, 3 of $^3B_{3g}$, 3 of $^1B_{3g}$, 1 of $^5B_{3g}$, 3 of $^3B_{2g}$, 3 of $^1B_{2g}$, 1 of $^5B_{2g}$, 5 of ^3A_u, 3 of ^1A_u, and 1 of ^5A_u,) in the trial wave function describing the electron plus target system. However, excitation cross sections are reported only for the four excited states ($a\ ^5\Sigma_u^-$, $A\ ^3\Pi_u$, b $^1\Delta_g$, and c $^1\Sigma_g^+$). Calculations were performed for doublet and quartet scattering states with $A_g, B_{2u}, B_{3u}, B_{1g}, B_{1u}, B_{3g}, B_{2g}$, and A_u symmetries. Continuum orbitals up to $l = 4$ (g partial wave) were included in the scattering calculation.

III. RESULTS

A. Elastic and inelastic total cross sections

The ground-state electronic configuration of B_2 has two unpaired π_u electrons. Due to a vacancy in the $2\pi_u$ orbital of the ground state of B_2, the scattering electron can occupy it, forming a stable anionic ground state of B_2^- with symmetry $^2\Pi_u$. In our 61-state model, we found an R-matrix pole at −49.193854 a.u. at R_e in the scattering symmetry $^2\Pi_u$ which is lower than the Hartree-Fock energy −49.1748 a.u. of ground state $X\ ^3\Sigma_g^-$ of B_2, which indicates the detection of an anionic bound state. We computed the value of vertical electronic affinity (VEA) from the bound-state calculation of B_2^- by including the continuum electron basis functions centered at the origin. The vertical electron affinity is equal to the difference between the total energy of the neutral molecule and its anion at the equilibrium geometry of the neutral molecule. We detect a stable bound state of B_2^- with $^2\Pi_u$ symmetry having configuration $1\sigma_g^2\ 2\sigma_g^2\ 1\sigma_u^2\ 2\sigma_u^2\ 1\pi_u^3$ with a VEA value of 0.518 eV (experimental value is 1.3 ± 0.4 eV [10]).

In Fig. 1, we have summed the contribution of doublet and quartet symmetries for 61-state calculation and compared with the 1-state results. In this figure, we show the contributions from each scattering symmetry of doublets and quartets separately. In doublets, we notice peaks at 1.45, 2.25, and 2.4 eV in the cross sections of $(^2A_u)\ ^2\Sigma_u^-$, $(^2B_{2u}/^2B_{3u})^2\Pi_u$ and $(^2B_{2g}/^2B_{3g})\ ^2\Pi_g$ symmetries, respectively. In quartets, we detected peaks at 1.6 and 4.26 eV in the cross sections of $(^4B_{2g}/^4B_{3g})^4\Pi_g$ and $(^4B_{1g})\ ^4\Sigma_g^-$ symmetries, respectively. The eigenphase sum corresponding to each symmetry shows a sudden jump of π radian centered at the same position, respectively. This jump is characteristic of a resonance. The resonance properties and types of these resonances are also given in Table III. We also compared the elastic cross section of SE (static exchange), SEP (static exchange plus polarization), and 1-state CI models. The SE model is unique whereas the SEP model depends upon the number of virtuals included in the calculations. In the SEP model, the effect of polarization is included by virtual excitation of a molecular orbital within the Hartree-Fock configuration to one of the unoccupied virtual orbitals available for a particular symmetry.

In Figs. 2–4 we show the inelastic cross sections from the ground state to the four physical states whose vertical excitation thresholds along with their quadrupole moments and the number of CSFs included in the CI expansion are given in Table II. We show the results of four excitation processes at the 61-state level. The cross section for higher excited states is less than $0.1 \times 10^{-16}\ cm^2$.

We have adopted a resonance fit procedure in which the eigenphase sum is fitted to the Breit-Wigner formula [14] with a quadratic dependence on the energy as background. In Fig. 2 we notice a sharp peak at 1.6 eV in the cross section of the $X\ ^3\Sigma_g^- - a\ ^5\Sigma_u^-$ transition. This resonance belongs to

TABLE II. Vertical excitation energies (VEEs in eV), quadrupole moments (Q_{20} in a.u.), and N the number of configuration state functions (CSFs) for the target states of B_2 at bond length $R_e = 3.18a_0$.

State	Present work	Ref. [7][a]	Ref. [8][b]	Ref. [9][c]	Present work	
$D_{2h}/D_{\infty h}$	(eV)	(eV)	(eV)	(eV)	Q_{20} (a.u.)	N
$X\ ^3B_{1g}/\mathrm{X}\ ^3\Sigma_g^-$	0.0				0.202	866
$1\ (^5A_u)/1\ ^5\Sigma_u^-$	0.096	0.227	0.14	0.222	0.856	330
$A\ ^3B_{2u}, ^3B_{3u}/\mathrm{A}\ ^3\Pi_u$	0.415	0.419	0.43	0.415	5.548	870
$b\ (^1A_g, ^1B_{1g}/b\ ^1\Delta_g$	0.796	0.572	0.64	0.575	0.168	714/566
$c\ (^1A_g)/c\ ^1\Sigma_g^+$	1.07	0.907	1.91	0.915	0.0235	714
$d\ ^1B_{2u}, ^1B_{3u}/d\ ^1\Pi_u$	1.328	1.13	1.22	1.12	5.5	610
$e\ (^1A_g)/e\ ^1\Sigma_g^+$	1.585	1.453	1.40	1.455	11.375	714
$1\ (^3A_u, ^3B_{1u})/1\ ^3\Delta_u$	1.858	1.591	1.64	1.589	1.193	884/866
$1\ (^3A_u)/1\ ^3\Sigma_u^-$	1.984	1.787	1.88	1.775	1.235	866
$1\ (^3B_{1u})/1\ ^3\Sigma_u^+$	2.184	2.047	1.98	2.051	1.132	884
$1\ ^3B_{2g}, ^3B_{3g}/1\ ^3\Pi_g$	2.444	2.045	2.04	2.038	4.03	870
$1\ (^1A_u)/1\ ^1\Sigma_u^-$	2.713	2.427	2.47	2.406		566
$2\ ^3B_{2g}, ^3B_{3g}/2\ ^3\Pi_g$	2.965	2.837	2.78	2.833	1.494	870
$1\ ^1B_{2g}, ^1B_{3g}/1\ ^1\Pi_g$	4.068	3.044	3.19	3.04		610
$1\ (^5A_g, ^5B_{1g}/1\ ^5\Delta_g$	4.206	3.902	3.77	3.900	3.753	330/258
$1\ (^5A_g)/1\ ^5\Sigma_g^+$	4.325	4.003	3.87	4.000	3.751	258
$2\ (^3A_u)/2\ ^3\Sigma_u^-$[d]	4.381	3.855	3.72	1.555	0.894	866
$1\ ^5B_{1g}/1\ ^5\Sigma_g^-$	4.638	4.581	4.48	4.587	4.214	330
$2\ (^3A_u, ^3B_{1u})/2\ ^3\Delta_u$	4.662		3.73	3.601	2.375	884/866
$2\ ^3B_{1g}/2\ ^3\Sigma_g^-$	4.765	4.448	4.29	4.438	3.586	866
$2\ (^3B_{1u})/2\ ^3\Sigma_u^+$	4.797	3.793	3.87		2.399	884
$2\ ^1B_{2g}, ^1B_{3g}/2\ ^1\Pi_g$	4.968	4.543	4.67	4.5	7.03	610
$1\ (^1A_u, ^1B_{1u})/1\ ^1\Delta_u$	4.986	4.346	4.56	4.304	1.31	566/664
$2\ ^3B_{2u}, ^3B_{3u}/2\ ^3\Pi_u$	5.074	4.324	4.28	4.316	5.074	870
$1\ ^5B_{2u}, ^5B_{3u}/1\ ^5\Pi_u$	5.157	4.618	4.54	4.618	2.626	286
$2\ (^1A_u)/2\ ^1\Sigma_u^-$	5.203		4.77		2.043	566
$2\ ^1B_{2u}, ^1B_{3u}/2\ ^1\Pi_u$	5.389	4.574	4.51		2.803	610
$1\ (^1B_{1u})/1\ ^1\Sigma_u^+$	5.715		5.32		1.765	664
$2\ (^1A_g, ^1B_{1g}/2\ ^1\Delta_g$	5.936		5.59		3.207	714/566
$3\ ^3B_{1g}/3\ ^3\Sigma_g^-$	5.944	5.421	5.54		3.345	866
$3\ (^1A_g)/3\ ^1\Sigma_g^+$	6.102	4.921	4.88		0.694	714
$^3B_{2g}, ^3B_{3g}/^3\Pi_g$	6.352				7.413	870
$3\ ^3B_{2u}, ^3B_{3u}/3\ ^3\Pi_u$	6.370	5.551	5.43		2.188	870
$1\ ^3A_g, ^3B_{1g}/1\ ^3\Delta_g$	6.395	5.665	5.79		4.089	834/866
$1\ (^3A_g)/1\ ^3\Sigma_g^+$	6.625		5.84		4.022	834
$3\ ^1B_{2g}, ^1B_{3g}/3\ ^1\Pi_g$	6.730		4.67		7.611	610
$1\ ^5B_{2g}, ^5B_{3g}/1\ ^5\Pi_g$	6.800	6.611	6.51	6.615	0.347	286
$^3B_{2u}, ^3B_{3u}/^3\Pi_u$	7.265				2.563	870
$(^3A_u)/^3\Sigma_u^-$	7.290				3.444	884
$4\ ^3B_{1g}/4\ ^3\Sigma_g^-$	7.312	5.580			4.059	866

[a] $R_e = 3.037a_0$.
[b] $R_e = 3.014a_0$.
[c] $R_e = 3.033a_0$.
[d] Experimental value (3.79 eV) [7].

$(^4B_{2g}/^4B_{3g})\ ^4\Pi_g$ symmetry, which resembles a symmetry with the peak in the elastic cross sections at same position. This resonance in the quartet state has no choice but to decay only to the triplet ground state. It is a shape resonance as it decays to ground state when the electron in virtual orbital (B_{2g}/B_{3g}) is removed. We also detected a small kink at 4.26 eV which belongs to $^4B_{1g}\ ^4\Sigma_g^-$ symmetry, which is not clearly seen in the cross sections. This resonance is also present in the elastic

TABLE III. Resonance properties of B_2 at bond length $R = 3.18a_0$.

Symmetry	E_r (eV)	Γ_r (eV)	Type of resonance
$\ldots 1b_{2u}^2 1b_{3u}/\ldots 1b_{2u} 1b_{3u}^2$: $^2\Pi_u(^2B_{2u}/^2B_{3u})$	2.25	0.5	Core-excited
$\ldots 1b_{2u} 1b_{3u}(b_{2g}/b_{3g})$: $^2\Pi_g(^2B_{2g}/^2B_{3g})$	2.4	0.785	Shape
$\ldots 1b_{2u} 1b_{3u}(1b_{1u})$: $^2\Sigma_u^-(^2A_u)$	1.45	0.3	Core-excited
$\ldots 1b_{2u} 1b_{3u}(b_{2g}/b_{3g})$: $^4\Pi_g(^4B_{2g}/^4B_{3g})$	1.6	0.72	Shape
$\ldots 1b_{2u} 1b_{3u}(a_g)$: $^4\Sigma_g^-(^4B_{1g})$	4.26	0.468	Shape

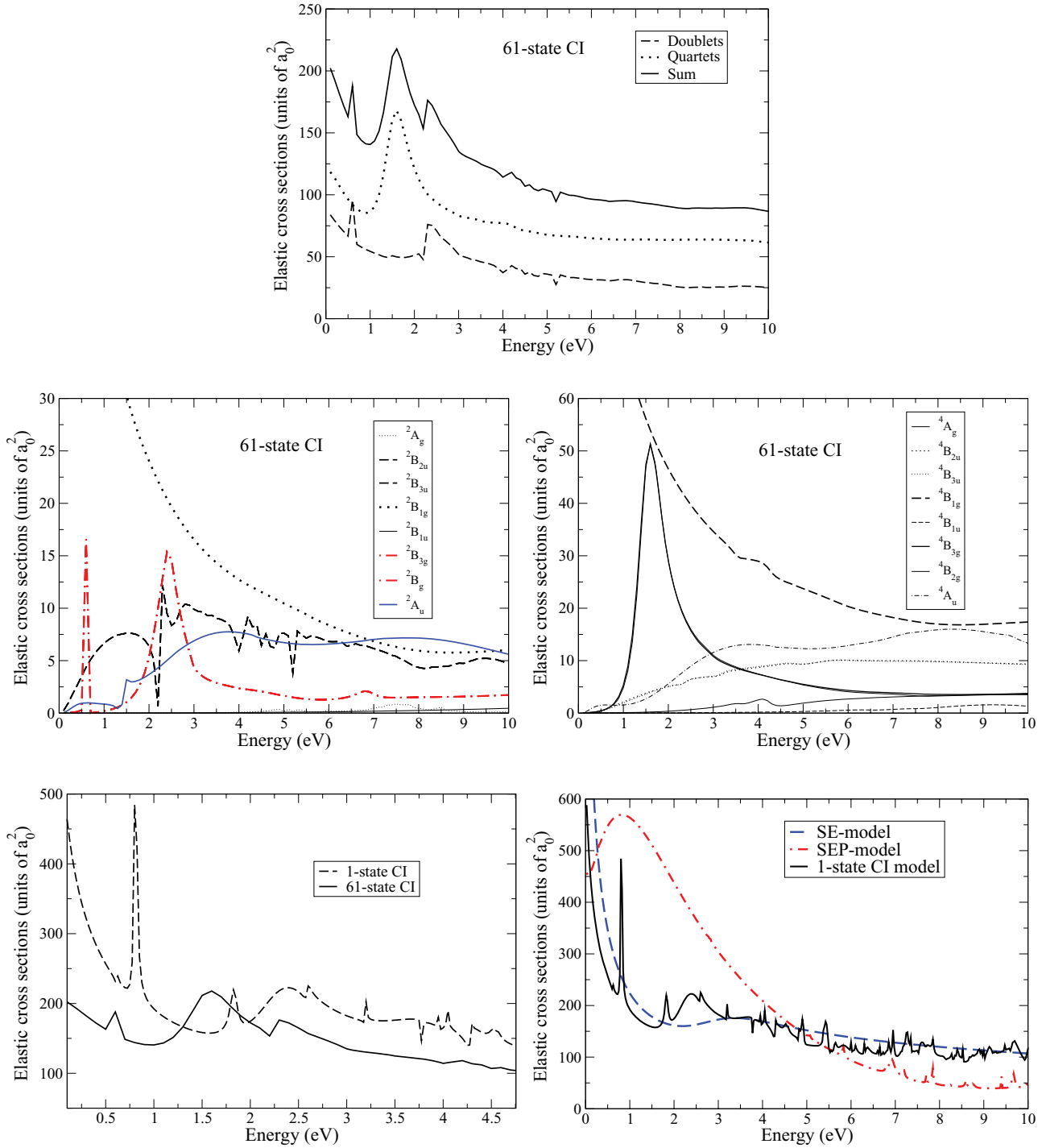

FIG. 1. (Color online) Elastic cross sections of the electron impact on the B_2 molecule for 61-state CI calculations at a bond length $R_e = 3.18a_0$. The 61-state CI results are compared with 1-state CI results. The elastic cross sections of SE, SEP, and 1-state CI models are also compared.

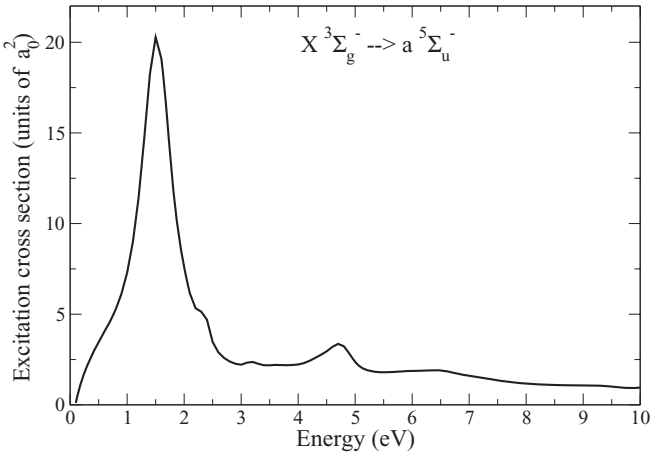

FIG. 2. Electron-impact excitation cross sections from the ground state: $X\ ^3\Sigma_g^-$ ($^3B_{1g}$) of the B_2 molecule to the excited states $a\ ^5\Sigma_u^-$.

region. When the electron in a_g orbital is removed, it decays to the ground state which gives rise to a shape resonance in this $^4\Sigma_g^-$ symmetry.

In Fig. 3 there are sharp peaks at 1.45 and 2.25 eV in the cross sections of the $X\ ^3\Sigma_g^- - A\ ^3\Pi_u$ transition. These resonances have widths of 0.3 and 0.5 eV, respectively, which belong to $(^2A_u)^2\Sigma_u^-$ and $(^2B_{2u}/^2B_{3u})\ ^2\Pi_u$ symmetries, respectively. The resonance in $^2\Sigma_u^-$ symmetry has three ways to decay into its parent state ($c\ ^1\Sigma_g^+$ at 1.07 eV, $b\ ^1\Delta_g$ at 0.796 eV, and ground state $^3\Sigma_g^-$) when the electron in virtual orbital B_{1u} is removed. The nearest lying excited state is present at 1.07 eV, so it has maximum probability to decay into its nearest excited state which is responsible for a core-excited shape resonance in $^2\Sigma_u^-$ symmetry. When the incoming electron is captured in the outer π_u orbital of the ground-state configuration, the other core-excited state resonance in $^2\Pi_u$ symmetry is formed, which is similar to the ground-state configuration of the B_2^- ion. It also has three ways to decay into its parent state but it has maximum probability to decay into its nearest excited state. The Born correction for this dipole allowed transition has been carried out to account for the

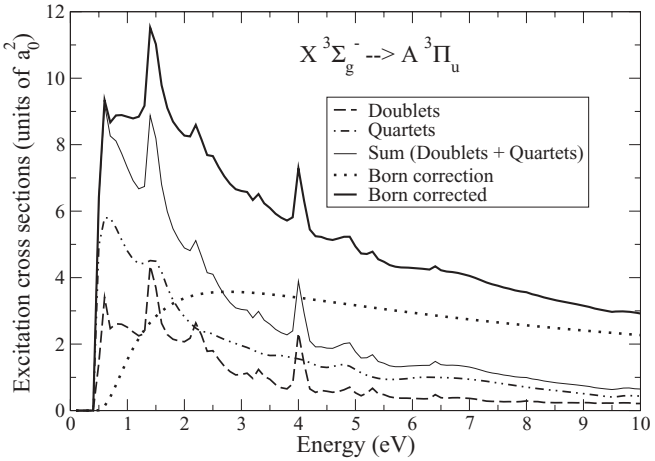

FIG. 3. Electron-impact excitation cross sections from the ground $X\ ^3\Sigma_g^-$ ($^3B_{1g}$) state of the B_2 molecule to the $A\ ^3\Pi_u$ states for the 61-state calculation.

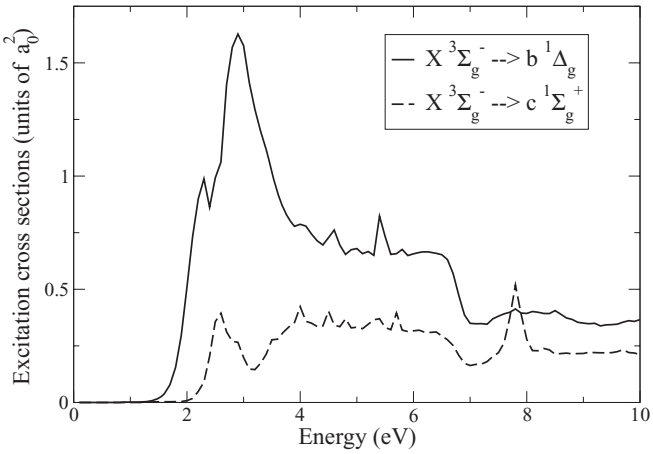

FIG. 4. Electron-impact excitation cross sections from the ground state: $X\ ^3\Sigma_g^-$ ($^3B_{1g}$) of the B_2 molecule to the excited states $b\ ^1\Delta_g$ and $c\ ^1\Sigma_g^+$.

contribution of partial waves [13] higher than the g wave up to which the R-matrix calculations are carried. There is a significant Born correction for this transition because of its low excitation threshold. The transition moments for the optically allowed transitions are given in Table IV. In the case of a dipole-allowed transition, the interaction responsible for the transition decreases slowly with the electron-molecule distance [13]. In this case the present Born-closure approach is also useful to obtain converged cross sections.

In Fig. 4, peaks are seen at 2.4 eV in the cross sections of the $X\ ^3\Sigma_g^- - b\ ^1\Delta_g$ and $X\ ^3\Sigma_g^- - c\ ^1\Sigma_g^+$ transitions. This resonance belongs to $(^2B_{2g}/^2B_{3g})\ ^2\Pi_g$ symmetry, which manifests itself in the elastic case as well. From Figs. 2 and 4 we have analyzed that both are shape resonances, in $^4\Pi_g$ symmetry and $^2\Pi_g$ symmetry, as they decay to ground state. According to Hund's rule, the resonance position of $^4\Pi_g$ symmetry lies lower than that of $^2\Pi_g$ symmetry.

B. Ionization cross section

Figure 5 shows electron-impact ionization cross sections of B_2 from threshold 9.54 to 5000 eV obtained by using the standard formalism of the binary-encounter-Bethe (BEB) model [18,19]. This formalism requires the binding energy and kinetic energy of each occupied orbital in a molecular-structure calculation. The ionization cross section rises from threshold to a peak value of 4.82 Å^2 at 53.72 eV and then shows

TABLE IV. Transition moments (in a.u.) of allowed transitions for B_2, at bond length $R_e = 3.18a_0$.

Transition	Transition moment (a.u.)
$X\ ^3\Sigma_g^- \rightarrow A\ ^3\Pi_u$	0.286
$X\ ^3\Sigma_g^- \rightarrow 2\ ^3\Pi_u$	0.234
$X\ ^3\Sigma_g^- \rightarrow 3\ ^3\Pi_u$	0.112
$X\ ^3\Sigma_g^- \rightarrow 1\ ^3\Sigma_u^-$	0.129
$X\ ^3\Sigma_g^- \rightarrow 2\ ^3\Sigma_u^-$	0.273
$X\ ^3\Sigma_g^- \rightarrow 3\ ^3\Sigma_u^-$	0.237

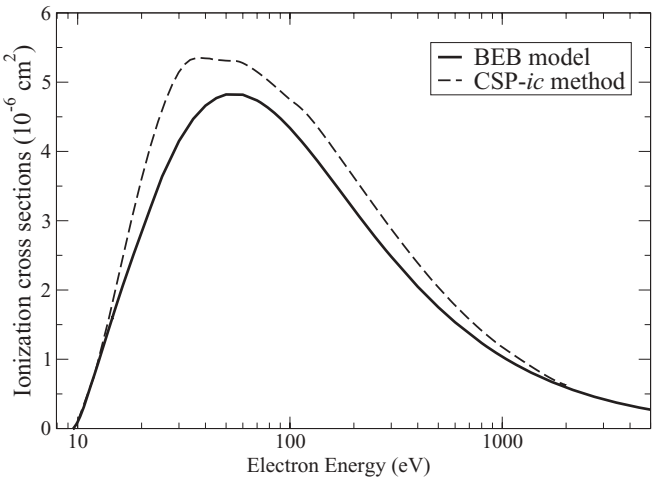

FIG. 5. Electron-impact BEB ionization cross sections of the B_2 molecule; dashed curve, complex spherical potential-ionization contribution method [11,12,31]; thick solid line, our BEB model results.

$\ln(E/E)$ behavior as E approaches higher values. We have also shown the results of the complex spherical potential-ionization contribution method [11,12,31] with a peak value of 5.4 Å^2 at 48.2 eV. This method is basically a potential scattering model in which the absorption potential is responsible for the loss of flux in all the inelastic channels including the excitation and ionization cross sections, and where ionization dominates. The molecular orbital data used in calculation of BEB cross section is given in Table V, which is generated at the SCF level. The BEB ionization cross section σ is obtained by summing over each orbital cross section σ_i, where

$$\sigma_i(t) = \frac{s}{t+u+1}\left[\frac{1}{2}\left(1-\frac{1}{t^2}\right)\ln t + \left(1-\frac{1}{t}\right) - \frac{\ln t}{t+1}\right], \tag{2}$$

where $t = T/B$, $u = U/B$, and $s = 4\pi a_0{}^2 N(R/B)^2$. Here R is the Rydberg energy, T is the kinetic energy of the incident electron, U is the orbital kinetic energy, N is the electron occupation number, and B is the binding energy of the orbital.

C. Differential cross section

The evaluation of the differential elastic cross sections (DCSs) provides a more stringent test for any theoretical model. The rotational excitation cross sections for electron impact on a neutral molecule can be calculated from the scattering parameters of elastic scattering in the fixed nuclei approximation provided the nuclei are assumed to be of infinite mass [32]. In this work the coupling of the electronic spin with the rotational motion, which is important for low-lying rotational states, is neglected and the spherical harmonics are used for the rotational states for simplicity. The rotational angular momentum quantum number is denoted by J. In particular, starting from an initial rotor state $J = 0$, the sum of all transitions from $J = 0$ level to a high enough J value for convergence is equivalent to the elastic cross section in the fixed nuclei approach. We have employed this methodology to extract rotationally elastic and rotationally inelastic cross sections from the K-matrix elements calculated in the one-state R-matrix model. The DCS for a general polyatomic molecule is given by the familiar expression

$$\frac{d\sigma}{d\Omega} = \sum_L A_L P_L(\cos\theta). \tag{3}$$

where P_L is a Legendre polynomial of order L. The A_L coefficients have already been discussed in detail [33].

The quantity $\frac{d\sigma}{d\Omega}$ for any initial rotor state $|Jm\rangle$ is given by the sum over all final rotor states $|J'm'\rangle$

$$\frac{d\sigma}{d\Omega} = \sum_{J'm'} \frac{d\sigma}{d\Omega}(Jm \to J'm'), \tag{4}$$

where J is the rotational angular momentum and m is its projection on the internuclear axis. We have calculated DCS by using the POLYDCS program of Sanna and Gianturco [34] that requires basic molecular input parameters along with K matrices evaluated in a particular scattering calculation. We have used this code to compute the DCS in the 1-state CI model. Since B_2 is an open-shell molecule having $X\,{}^3\Sigma_g^-$ as its ground state, the spin coupling between this target state and the spin of the incoming electron allows two spin-specific channels, namely, the doublet (D) and quartet (Q) couplings. The spin-averaged DCSs for elastic electron scattering from the B_2 molecule are calculated by using the statistical weight 2/6 for doublet and 4/6 for quartet scattering channels. We then use Eq. (3) as follows to calculate DCS:

$$\frac{d\sigma}{d\Omega} = \frac{1}{3}\left[2\left(\frac{d\sigma}{d\Omega}\right)^Q + \left(\frac{d\sigma}{d\Omega}\right)^D\right], \tag{5}$$

where $(\frac{d\sigma}{d\Omega})^{Q,D}$ represent DCSs for quartet and doublet cases, respectively.

In Fig. 6 we show the spin-averaged DCS calculated in the 1-state R-matrix model at different energies. In this figure we also show the DCSs at 4 eV for state-to-state rotational components of the DCS for initial state $J = 0$ to final state $J' = 0,2,4$. Since the electronic part of the wave function of the ground state of B_2 is antisymmetric, therefore the rotational part of the nuclear wave function is symmetric corresponding to even values of J because the boron nucleus is a fermion. The odd values of J do not exist and in our calculations the numerical error is less than 0.1×10^{-16} cm^2/sr. Besides this, the data on DCS are further used to calculate the elastic momentum-transfer cross section (MTCS) that shows the importance of backward angle scattering due to the weight

TABLE V. B_2 molecular orbital binding and average kinetic energies for DZP basis set at equilibrium geometry. $|B|$ is binding energy (eV), U is kinetic energy (eV), and N is occupation number.

Molecular orbital	$\lvert B\rvert$ (eV)	U (eV)	N
$1\sigma_g(1a_g)$	209.80	297.17	2
$1\sigma_u(1b_{1u})$	209.78	297.46	2
$2\sigma_g(2a_g)$	19.07	28.92	2
$2\sigma_u(2b_{1u})$	10.09	26.95	2
$1\pi_u(1b_{2u})$	4.77	18.07	1
$1\pi_u(1b_{3u})$	4.77	18.07	1

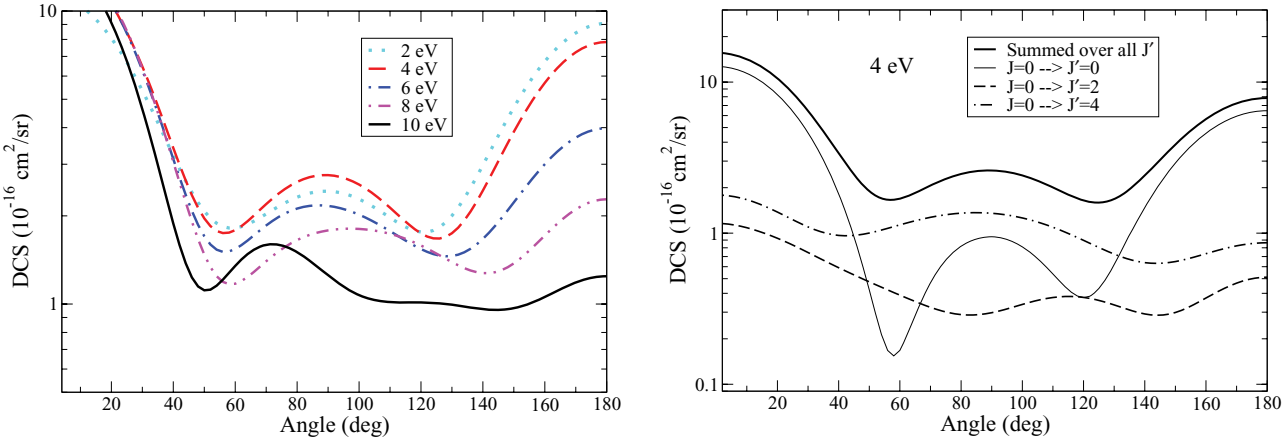

FIG. 6. (Color online) Differential cross sections at 2, 4, 6, 8, and 10 eV (with spin-average) for the 1-state CI model at R_e. DCSs at 4 eV are for state-to-state rotational components of DCS for initial state $J = 0$ to final state $J' = 0,2,4$.

factor $2\pi \sin\theta(1 - \cos\theta)\, d\theta$ which has a maximum value of $\theta = 120^\circ$. These are calculated in the 1-state CI model with spin-averaging. MTCS provides a useful input in solving the Boltzmann equation for the electron distribution function. The MTCS is useful in the study of electrons drifting through a molecular gas. When a swarm of electrons travels through a molecular gas under the influence of an electric field, several transport observables such as diffusion coefficient D and mobility μ can be obtained if we have a knowledge of the momentum-transfer cross sections. In Fig. 7, we show the calculated MTCSs at different energies for electron collision with a B_2 molecule. The inelastic transitions also occur in the energy range where the MTCS is shown, and the inelastic MTCSs are also important in determining the electron transport phenomena.

D. Effective collision frequency of electrons

We evaluated two types of the effective electron-B_2 collision frequency $\langle v\rangle$ and $\bar{v}^{-1}$ using the MTCS $[Q^{(m)}(v)]$ data [35,36]. These are given by the following expressions in which it is assumed that the electrons follow a Maxwell-Boltzmann distribution:

$$\langle v\rangle = \frac{8}{3\pi^{1/2}} n_e \left(\frac{m_e}{2k_b T_e}\right)^{5/2} \int_0^\infty v^5 Q^{(m)}(v) \times \exp\left(\frac{-m_e v^2}{2k_b T_e}\right) dv, \tag{6}$$

$$\bar{v}^{-1} = \frac{8}{3\pi^{1/2} n_e} \left(\frac{m_e}{2k_b T_e}\right)^{5/2} \int_0^\infty \frac{v^3}{Q^{(m)}(v)} \times \exp\left(\frac{-m_e v^2}{2k_b T_e}\right) dv, \tag{7}$$

where m_e and T_e are the electron mass and temperature, respectively, k_b is Boltzmann's constant, v is the velocity, n_e is the number density of the gas particles, and T_e is electron temperature. When $Q^{(m)}(v)$ is proportional to v^{-1}, the two effective collision frequencies $\langle v\rangle$ and $\bar{v}$ agree. In Fig. 8, we show both types of effective collision frequencies as a function of electron temperature. Note that $\langle v\rangle$ lies higher than $\bar{v}$ in the entire electron temperature range. These collision frequencies are related to transport properties such as the mean free path, mobilities, and diffusion coefficients.

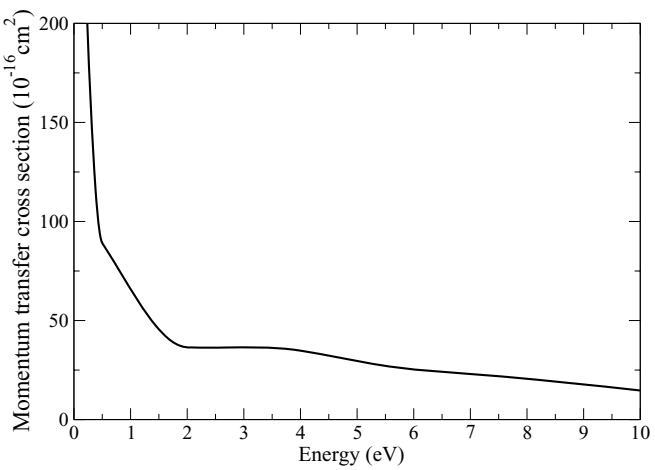

FIG. 7. MTCS at different energies with the spin average of the B_2 molecule ground state at the 1-state CI level.

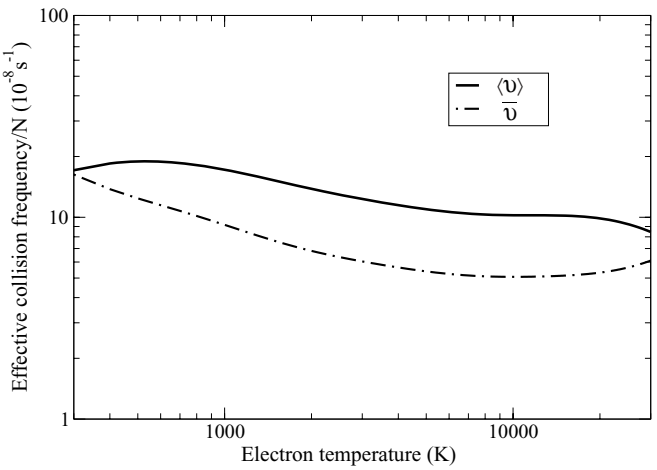

FIG. 8. Effective collision frequency as a function of electron temperature.

E. Scattering length

We have also evaluated scattering length in our study of electron impact on the B_2 molecule. In this procedure we included only the s wave for the scattering electron. The scattering length is given by

$$a = \frac{-\tan\delta_0}{k}, \quad k \to 0, \tag{8}$$

where δ_0 is the eigenphase sum corresponding to the energy ($E = 0$). In practice, we chose $E = 0.025$ eV to compute a. Here k is the wave number of the scattering electron.

We calculated the scattering length separately for doublets (a_D) and quartets (a_Q); the spin-averaged scattering length is given by

$$a = \left[\tfrac{1}{3}({a_D}^2 + 2{a_Q}^2)\right]^{1/2}. \tag{9}$$

We obtained the value of $6.8a_0$ for the scattering length. Then we evaluated the cross section $\sigma = 4\pi a^2$ corresponding to this scattering length which is equal to $578.04a_0^2$, this result is comparable with the cross section $587.77a_0^2$ at same energy ($E = 0.025$ eV) coming from direct calculation (R-matrix method). In our SEP model we used the complete active space to include the polarization effects. Our results in the SEP model agree with the 1-state CI model as expected. The scattering length evaluated in the SEP model is $6.2a_0$ which is in good agreement with that obtained in the 1-state CI model ($6.8a_0$).

IV. CONCLUSIONS

We have carried out a detailed study of electron impact on the B_2 molecule, using the R-matrix method. The results of the static exchange, correlated 1-state, and 61-state close-coupling approximations are presented. Our target calculations give reasonable agreement with the calculated vertical excitation spectrum of Langhoff and Bauschlicher [7], Hachey *et al.* [8], and Muller *et al.* [9]. We investigated five resonances: two in the excitation cross sections of $A\,^3\Pi_u$, two in the excitation cross sections of $a\,^5\Sigma_u^-$, and one in both $b\,^1\Delta_g$ and $c\,^1\Sigma_g^+$ excited states. We detected a stable bound state of B_2^-, with a vertical electronic affinity value of 0.518 eV. We also reported the quadrupole moment for each state. The data generated for MTCS were employed to calculate collision frequencies, which are useful to obtaining the mean free path. The ionization cross sections were calculated in the binary-encounter-Bethe model, which may be useful to experimentalists. We also evaluated the scattering length of the B_2 molecule, which is equal to $6.8a_0$.

[1] J. Niu, B. K. Rao, and P. Jena, J. Chem. Phys. **107**, 132 (1997).
[2] D. Meinkohn, Combust. Flame **59**, 255 (1985).
[3] A. F. Douglas and G. Herzberg, Can. J. Res. A **18**, 165 (1940).
[4] M. Dupuis and B. Liu, J. Chem. Phys. **68**, 2902 (1978).
[5] P. J. Bruna and J. S. Wright, J. Chem. Phys. **91**, 1126 (1989).
[6] P. J. Bruna and J. S. Wright, J. Chem. Phys. **94**, 1774 (1990).
[7] S. R. Langhoff and C. W. Bauschlicher, Jr., J. Chem. Phys. **95**, 5882 (1991).
[8] M. Hachey, S. P. Karna, and F. Grein, J. Phys. B **25**, 1119 (1991).
[9] T. Muller, M. Dallos, H. Lischka, Z. Dubrovay, and P. G. Szalay, Theor. Chem. Acc. **105**, 227 (2001).
[10] http://cccbdb.nist.gov/.
[11] K. N. Joshipura, M. Vinodkumar, C. G. Limbachiya, and B. K. Antony, Phys. Rev. A **69**, 022705 (2004).
[12] K. N. Joshipura, S. Gangopadhyay and G. Vaishnav Bhushit, J. Phys. B **40**, 199 (2007).
[13] Y. Itikawa, Theor. Chem. Acc. **105**, 123 (2000).
[14] J. Tennyson and C. J. Noble, Comput. Phys. Commun. **33**, 421 (1984).
[15] L. A. Morgan, C. J. Gillan, J. Tennyson, and X. Chen, J. Phys. B **30**, 4087 (1997).
[16] L. A. Morgan, J. Tennyson, and C. J. Gillan, Comput. Phys. Commun. **114**, 120 (1998).
[17] J. Tennyson, J. Phys. B **29**, 1817 (1996).
[18] Y. K. Kim and M. E. Rudd, Phys. Rev. A **50**, 3954 (1994).
[19] W. Hwang, Y. K. Kim, and M. E. Rudd, J. Chem. Phys. **104**, 2956 (1996).
[20] C. W. McCurdy and T. N. Rescigno, Phys. Rev. A **39**, 4487 (1989).
[21] P. G. Burke and K. A. Berrington, *Atomic and Molecular Processes: An R-matrix Approach* (IOP, Bristol, UK, 1993).
[22] C. J. Gillan, J. Tennyson, and P. G. Burke, in *Computational Methods for Electron-Molecule Collisions,* edited by W. M. Huo and F. A. Gianturco (Plenum, New York, 1995).
[23] J. Tennyson, Phys. Rep. **491**, 29 (2010).
[24] P. G. Burke, *R-Matrix Theory of Atomic Collisions: Application to Atomic, Molecular and Optical Processes* (Springer, New York, 2011).
[25] K. L. Baluja, P. G. Burke, and L. A. Morgan, Comput. Phys. Commun. **27**, 299 (1982).
[26] L. A. Morgan, Comput. Phys. Commun. **31**, 419 (1984).
[27] B. M. Nestmann, K. Pfingst, and S. D. Peyerimhoff, J. Phys. B **27**, 2297 (1994).
[28] J. Tennyson, J. Phys. B **29**, 6185 (1996).
[29] A. Faure, J. D. Gorfinkiel, L. A. Morgan, and J. Tennyson, Comput. Phys. Commun. **144**, 224 (2002).
[30] T. H. Dunning and P. J. Hay, in *Methods of Electronic Structure Theory*, edited by H. F. Schaefer (Plenum, New York, 1977), Vol. 2.
[31] M. Vinodkumar (private communication).
[32] E. S. Chang and A. Temkin, Phys. Rev. Lett. **23**, 399 (1969).
[33] F. A. Gianturco and A. Jain, Phys. Rep. **143**, 347 (1986).
[34] N. Sanna and F. A. Gianturco, Comput. Phys. Commun. **114**, 142 (1998).
[35] Y. Itikawa, Phys. Fluids **16**, 831 (1973).
[36] I. P. Shkarofsky, Can. J. Phys. **39**, 1619 (1961).